

An Automated Solar Shading Calculator

M.K.Dennis
Centre for Sustainable Energy Systems
Australian National University
Canberra ACT 0200
AUSTRALIA
Telephone: +61 02 6125 3976
Facsimile: +61 02 6125 0506
E-mail: mike@faceng.anu.edu.au

The author has been supported by an ACRE Postgraduate Research Scholarship

Abstract

Designers of solar systems often estimate solar performance based on the site latitude, averaged weather profiles and the characteristics of the solar system. This paper presents a means of integrating this predicted insolation with losses due to direct shading of the solar system. An automated artificial horizon capture and processing system is presented. This artificial horizon is then compared to the solar coordinates at high time resolution so that shading losses may be summarised over an arbitrary period. The approach is applicable to photovoltaics, solar thermal and building applications. A subroutine has been produced for the popular TRNSYS modelling package.

1 INTRODUCTION

Solar engineers will be familiar with the sunpath diagram as a useful design aid to predict the occurrence of solar gain on a system. Obstructions to the solar path may be tediously measured using surveying equipment and superimposed upon the sunpath diagram for the locale of the system and the times of shading deduced henceforth. This paper provides an alternative partially automated means of capturing the artificial horizon information and its subsequent processing to provide meaningful data regarding insolation energy losses due to shading of the system

1.1 Nomenclature

L	Luminance or brightness coefficient ($0.0 \leq L \leq 1.0$)
R	Red colour intensity coefficient ($0.0 \leq R \leq 1.0$)
G	Green colour intensity coefficient ($0.0 \leq G \leq 1.0$)
B	Blue colour intensity coefficient ($0.0 \leq B \leq 1.0$)
α	Solar azimuth measured in degrees from true North (deg)
β	Solar altitude measured in degrees from the vertical (deg)
β_a	Artificial horizon elevation measured in degrees from the horizontal (deg)
d	Ordinal day of year
K	Solar constant (W/m^2)
H	Beam insolation incident on Earth's Surface at locale of solar system (W/m^2)
M	Air mass

2. Horizon Capture

Capturing the Artificial Horizon

A low resolution digital camera is used to capture a sequence of images of the horizon.

The digital camera is mounted on a level tripod and is actuated by an azimuthal drive. This drive consists of a stepper motor controlled electronically to move exactly 60 degrees in an azimuthal direction upon the push of a button. After each movement, a digital photograph is taken and stored in the camera's memory. Use of the drive allows six images to be captured and thus cover the entire horizon. This procedure takes about 10 minutes.

The camera used had a field of view of approximately 64 degrees in azimuth and 48 degrees in altitude. The tripod is aligned so that the bottom of the image represents an elevation of 0 degrees relative to the horizontal. For distant horizons, this elevation represents the elevation of the horizon. The images are later cropped in width to be exactly 60 degrees wide so that they align with neighbouring images.

Most camera lenses suffer a degree of non-linearity near the edges of the image, often referred to as the pin cushion effect. To account for this, an image of an angular grid (drawn on a cardboard screen) was taken and superimposed upon an actual angular grid. Assuming that the lens is a point focus device, one may readily observe any image distortion. The image distortion was found to be significant near the boundaries of the image. Although some of these areas are cropped during processing, no further corrective action was taken. The linearisation of a digital image is not a trivial matter considering that the artificial horizon is to be detected on a pixel by pixel basis. It is therefore important to understand quantitatively the errors that might be introduced by this approximation. Analysis of the grid image produces the error quantities listed in Table 1 for this particular camera.

<i>Elevation (deg)</i>	<i>Azimuth Error (deg)</i>	<i>Altitude Error (deg)</i>
0	±0.2	0.5
10	±0.1	0.4
20	±0.0	0.2
25	±0.0	0.0
30	±0.0	-0.2
40	±0.1	-0.4
50	±0.2	-0.5

Table 1. Errors Introduced by Camera Lens Distortion

The algorithm uses an angular resolution of one degree in azimuth and altitude for its calculations. Thus the camera must have a frame at least 60 pixels wide. Most digital cameras use a minimum resolution of 640*480 pixels and this extra resolution is utilised by the discrimination algorithm. It is not uncommon for pixels in CCD devices to fail and so an average of a number of neighbouring pixels is used in the discriminator.

Processing the Images.

Each image is downloaded from the camera to the PC using the software provided with the camera. Each picture is decompressed from JPEG form into a bitmap form known as Device Independent Bitmap (DIB). This format allows inspection of individual pixel elements.

Processing the images requires detecting the difference between sky and the artificial horizon, commonly defined by trees and buildings. Colour alone is a poor discriminator in many circumstances and it has been found better to use luminance for this purpose. Once converted to gray scale, the luminance or brightness of a colour is given by the relation

$$L = 0.299 R + 0.589 G + 0.114 B$$

For the purpose of selecting the horizon, the sky must be bright and objects representing the horizon must be dark. It may be beneficial to modify the colour balance of the luminance signal to achieve greater contrast. Reasonable contrast is given with the following luminance composition

$$L = 0.3 R + 0.4 G + 0.3 B$$

An algorithm may now scan each image from top to bottom, one column of pixels at a time, searching for this change from light to dark luminance change that represents the artificial horizon. Through trial and error it was found that a weighted average of groups of three neighbouring vertical pixels gave best differentiation and best tolerance to false indication of the horizon. This method was good enough to allow deciduous trees to be detected in winter.

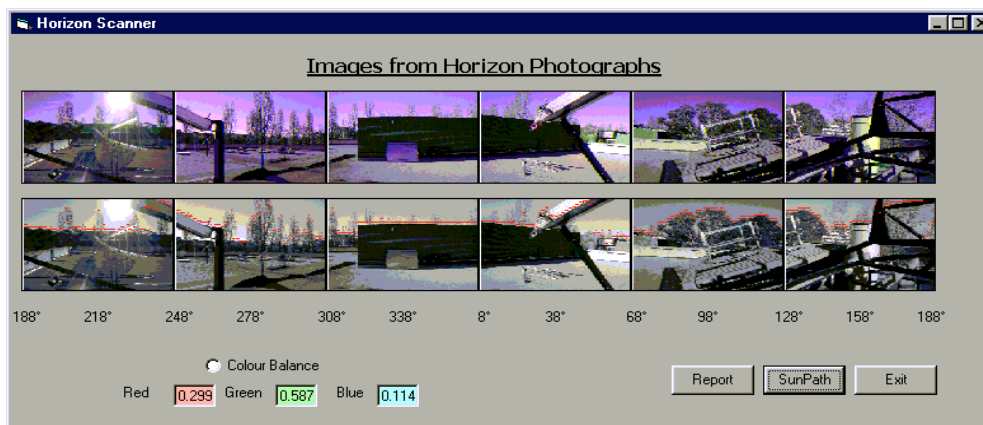


Figure 1. Sample photographs of the artificial horizon from a test site

The top row of colour images show good colour contrast between sky and ground. The lower set shows the luminance signal with the horizon detected and plotted as a red line.

The elevation and azimuth of every object forming the artificial horizon may thus be recorded after suitable scaling of the pixel density.

Calculating the Timing of Shading Events

The solar coordinates may be obtained from a number of algorithms given the local Latitude, Longitude and time (Rabl, 1985). Solar coordinates in this paper are represented by the two quantities, azimuth and altitude. The locus of the sun in this coordinate system may be plotted for a range of days of year and times of day, giving rise to a *Sunpath Diagram* that may be represented in polar form (Figure 2) or cartesian form (Figure 3).

The artificial horizon may also be plotted on a sunpath diagram. The region of overlap between the area outside of this trace and the solar coordinates represents a period of shading at the represented location. It is convenient to write a computer algorithm to locate each shading event.

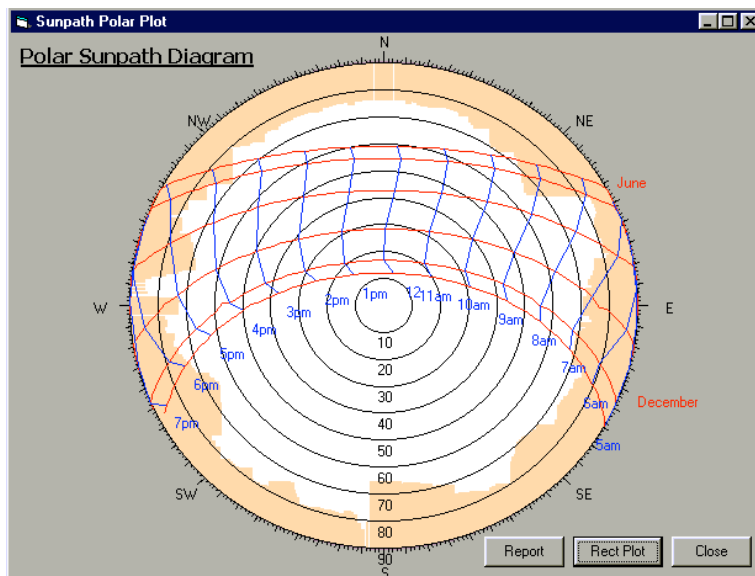


Figure 2. Sunpath Polar Plot

A polar plot of the sunpath diagram for Canberra. Note the profile of the artificial horizon plotted as the shaded area near the periphery of the diagram

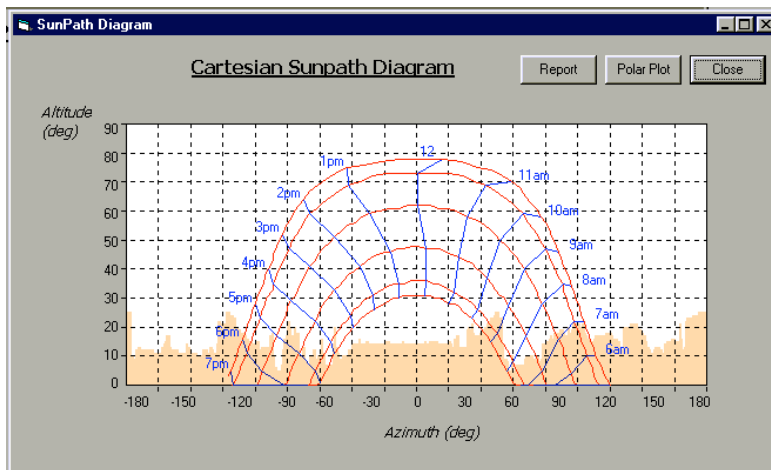


Figure 3. Sunpath Cartesian Plot

This is a rectangular plot of the sunpath diagram for Canberra. Note the profile of the artificial horizon plotted as the shaded area near the bottom of the diagram

Predicting Clear Sky Insolation

The above results use the solar coordinates as the basis of predicting the timing of shading on the solar system. Although useful in itself, the timing of shading may then be used to predict solar energy loss due to the artificial horizon, provided that temporal breakdown of insolation is known.

A commonly used approximation for the insolation reaching the surface of the Earth relies on two calculations:

1. Insolation incident upon the Earth's upper atmosphere which varies with the distance between the Earth and Sun (i.e. seasonal). This is approximated by the Solar Constant, K .

$$K = 1373 (1 + 0.033 \cos (2 \pi (d + 10) / 365.25)) \quad \text{W/m}^2$$

2. Calculation of the path length of direct radiation from the sun through the Earth's atmosphere to the locale of interest. This is referred to as the Air Mass, M

$$M = 1 / \cos (\theta)$$

This approximation ignores a small change in insolation due to atmospheric refraction at low solar elevation. This is usually ignored since the sun's intensity is low at these times, however this is when shading is most likely to occur. Thus the empirical refraction correction (Hu and White, 1983) is included.

$$M = (1 / \cos (\theta) + 0.15 (3.885 + \theta)^{-1.253}) * \exp (-0.0001184 * \text{Altitude})$$

This equation accounts for atmospheric absorption and the altitude of the site but ignores changes in air pressure and temperature

Thus the direct beam insolation incident on a two axis tracking collector with known Latitude and time can be found from the expression

$$H = K * 0.7^{\wedge} (M^{\wedge} 0.678) \quad \text{W/m}^2$$

This insolation may be readily modified into insolation incident upon a flat plate of known orientation or other mode of tracking (Rabl, 1985)

Incorporating Weather Effects

The reader would recognise that local weather conditions will have a major influence on the amount of solar energy lost as a result of shading effects. To incorporate weather effects, the artificial horizon information is imported into a modeling program that utilises weather data. The popular TRNSYS (Klein, 1996) modelling package is used in this case. TRNSYS uses a format of weather data known as Typical Meteorological Year (TMY) which is a representative average weather dataset of one hour time resolution. A TMY file was located for the test locale (*Morrison et al, 1988*)

A new TRNSYS Type was constructed that essentially acts as a digital filter on the beam insolation signal from the existing TRNSYS Radiation Processor. The diffuse radiation is unaffected. This Type connects between the Radiation Processor Type and the Solar Collector Type in the system simulation. The algorithm is simply:

```
IF [ (θ/2 - θ) > θ(θ) ] THEN
    H=K*M
ELSE
    H=0
ENDIF
```

A simple TRNSYS model was constructed to give quantitative results for average annual weather conditions at the surveyed site in Canberra. These results may be tabulated by arbitrary time interval. Monthly summary results are presented in Table 1.

<i>Month</i>	<i>Clear Sky Insolation (kWh)</i>	<i>Actual Insolation (kWh)</i>	<i>Shaded Insolation (kWh)</i>
<i>January</i>	344	259	249
<i>February</i>	287	195	182
<i>March</i>	280	209	190
<i>April</i>	229	139	128
<i>May</i>	198	111	94
<i>June</i>	172	109	96
<i>July</i>	188	95	81
<i>August</i>	222	146	130
<i>September</i>	256	157	149
<i>October</i>	306	196	174
<i>November</i>	327	219	204
<i>December</i>	352	212	192
<i>TOTAL</i>	3163	2050	1860

Table 2. A Useful Summary of the Effects of Shading at the Test Site

The simulation results for the test site in Canberra indicate an annual loss of radiation of around 9% due to shading from nearby buildings and trees. The sunpath diagram may be used to retrospectively identify the objects causing the greatest losses by locating the objects in the original images using the azimuth as an index.

3 CONCLUSION

A simple method for real world analysis of shading effects on solar systems has been presented. The system provides the engineer with a simple tool to quantitatively predict the shading effects of nearby obstructions. A new subroutine is available to TRNSYS users who wish to incorporate this addition to their models.

4 ACKNOWLEDGEMENTS

The work described in this paper has been supported by the Australian Cooperative Research Centre for Renewable Energy (ACRE). ACRE's activities are funded by the Commonwealth's Cooperative Research Centres Program.

5 REFERENCES

- Duffie J.A. and Beckman W.A. (1991) *Solar Engineering of Thermal Processes*, 2nd edn, pp.54-59. Wiley Interscience, New York.
- Klein (1996) *A Transient System Simulation Program*, Solar Energy Laboratory, University of Wisconsin, Madison.
- Morrison G.L. and Litvak A. (1988) *Condensed Solar Radiation Data Base for Australia*, Solar Thermal Energy Lab, University of New South Wales, Australia
- Rabl A. (1985) *Active Solar Collectors and Their Applications*, pp28-35, Oxford University Press, New York
- Hu C. and White R.M. (1983) *Solar Cells: From Basics to Advanced Systems* McGraw Hill, New York